

Acute Delivery of EphA4-Fc Improves Functional Recovery after Contusive Spinal Cord Injury in Rats

Mark Damien Spanevello,^{1,2} Sophie Ines Tajouri,¹ Cornel Mirciov,¹ Nyoman Kurniawan,³ Martin John Pearse,⁴ Louis Jerry Fabri,⁴ Catherine Mary Owczarek,⁴ Matthew Philip Hardy,⁴ Rebecca Anne Bradford,⁴ Melanie Louise Ramunno,⁴ Ann Maree Turnley,⁵ Marc Jan Ruitenber,^{1,6} Andrew Wallace Boyd,^{2,7} and Perry Francis Bartlett¹

Abstract

Blocking the action of inhibitory molecules at sites of central nervous system injury has been proposed as a strategy to promote axonal regeneration and functional recovery. We have previously shown that genetic deletion or competitive antagonism of EphA4 receptor activity promotes axonal regeneration and functional recovery in a mouse model of lateral hemisection spinal cord injury. Here we have assessed the effect of blocking EphA4 activation using the competitive antagonist EphA4-Fc in a rat model of thoracic contusive spinal cord injury. Using a ledged tapered balance beam and open-field testing, we observed significant improvements in recovery of locomotor function after EphA4-Fc treatment. Consistent with functional improvement, using high-resolution *ex vivo* magnetic resonance imaging at 16.4T, we found that rats treated with EphA4-Fc had a significantly increased cross-sectional area of the dorsal funiculus caudal to the injury epicenter compared with controls. Our findings indicate that EphA4-Fc promotes functional recovery following contusive spinal cord injury and provides further support for the therapeutic benefit of treatment with the competitive antagonist in acute cases of spinal cord injury.

Key words: EphA4; magnetic resonance imaging; neurotrauma; spinal cord injury

Introduction

INJURIES TO THE SPINAL CORD result in the apoptosis and necrosis of damaged nervous tissue as well as damage to ascending and descending myelinated nerve tracts. Subsequent to the primary damage caused by the initial mechanical injury, further cell death and axonal damage are caused by excitotoxic, ischemic, and inflammatory cascades. As the adult mammalian central nervous system (CNS) has limited inherent capacity to regenerate and restore functional connectivity across the injury site, traumatic spinal cord injury (SCI) often results in permanent deficits in movement, sensation, and autonomic functions at and below the level of the injury. There are now numerous reports showing that repulsive guidance factors are upregulated following SCI. At the lesion site, factors such as Nogo (Reticulon 4), repulsive guidance molecule, chondroitin sulphate proteoglycans, semaphorins, slits, and Eph receptors are thought to actively inhibit the regeneration of CNS axons, and, therefore, are current targets for possible therapies to treat SCI.^{1–6}

The Eph:ephrin (receptor:ligand) system is known to play an important role in spinal cord development as well as injury.

Members of both the Eph receptor and ephrin ligand families are divided into two subgroups (A and B) with each group showing high intra- but not inter-class affinity.^{7,8} Of the receptors, EphA4 is notable, as it is capable of interacting with ligands from both subgroups.^{7,8} EphA4 is known to be involved in the formation of the major commissures of the brain, patterning of the corticospinal tract, and creation and/or wiring of the central pattern generator.^{9–11} Previous research has shown that EphA4 and its ligands are upregulated following injury to the spinal cord and act to prevent axonal regeneration.^{12–15} We, and others, have found using rodent models of transectional SCI, that either genomic deletion or competitive antagonism of EphA4 leads to axonal regeneration and significant functional recovery.^{16–18} Given the therapeutic potential of EphA4 antagonism, we have expanded our investigation of EphA4-Fc treatment to a rat model of contusive SCI: a model more relevant to human SCI, as it replicates many pathological features typical of crush or fracture injuries, such as acute edema and chronic syrinxomyelia.

Magnetic resonance imaging (MRI) is an integral component of the diagnosis and management of human SCI, as it provides a

¹Queensland Brain Institute, ³Centre for Advanced Imaging, and Schools of ⁶Biomedical Sciences and ⁷Medicine, The University of Queensland, Brisbane, Queensland, Australia.

²Queensland Institute of Medical Research, Brisbane, Queensland, Australia.

⁴CSL Limited, Melbourne, Victoria, Australia.

⁵Centre for Neuroscience, The University of Melbourne, Melbourne, Victoria, Australia.

noninvasive method to assess the severity of the injury and identify many of the associated pathological changes, including atrophy, hemorrhage, edema, and cyst/syrinx formation.^{19–21} It is also a valuable tool for assessment of animal models of SCI, as the data can be easily translated and compared with human SCI MRI data. Diffusion tensor imaging (DTI), a method to quantify the magnitude and direction of water movement, is increasingly being used to examine pathway integrity after traumatic injuries and other degenerative diseases affecting the CNS.^{22,23} Changes detected by MRI and DTI following SCI are thought to provide good correlation with anatomical, immunohistochemical, and behavioral observations.^{24–26}

In the present study, we delivered the recombinant fusion protein EphA4-Fc to rats following a moderate force-controlled (150 kdyne) contusive injury to the lower thoracic spinal cord. Our results revealed that EphA4-Fc promotes improvements in both locomotor performance and spinal cord structure after contusive injury, providing further evidence that EphA4-Fc is a therapeutic candidate for the treatment of human SCI.

Methods

Protein expression and purification

Ephrin A4-Fc, comprised of the extracellular domain of human ephrin A4 (amino acids 1–166 of NP_005218.1) fused to the Fc region of human IgG1 (amino acids 99–330 of P01857.1), was generated and purified as previously described.^{18,27} To minimize the possibility of an Fc-mediated response in the rat, we used a recombinant Fc protein, which consisted of the extracellular domain of human EphA4 (amino acids 1–546 of NP_004429.1) fused to the human Fc domain of IgG4 (amino acids 99–327 of P01861.1). EphA4-Fc was cloned into the mammalian expression vector pcDNA3.1 (Invitrogen, Life Technologies). The nucleotide sequence of the construct was verified by sequencing both strands using BigDye™ Terminator Version 3.1 Ready Reaction Cycle Sequencing and an Applied Biosystems 3130xl Genetic Analyzer. Large-scale preparations of plasmid DNA were conducted using QIAGEN Plasmid Giga Kits according to the manufacturer's instructions.

Transient transfections of the EphA4-Fc expression plasmid using FreeStyle™ 293-F cells were performed using 293fectin™ transfection reagent (Invitrogen, Life Technologies) according to the manufacturer's instructions. Cells (1000 mL) were transfected at a final concentration of 1×10^6 viable cells/ml and incubated in a 2L Cellbag (GE Healthcare Life Sciences) for 6 days at 37°C in 8% CO₂ on a 2/10 Wave Bioreactor system or 20/50 (GE Healthcare). The culture conditions were 35 rocks/min with an angle of 8°. Pluronic F68 (GIBCO, Life Technologies), to a final concentration of 0.1% v/v, was added 4 h post-transfection. At 24 h post-transfection, cell cultures were supplemented with LucraTone Lupin (Millipore) to a final concentration of 0.5 % v/v. The cell culture supernatants were harvested by centrifugation at 2500 rpm and were then passed through a 0.45 μm filter (Nalgene) prior to purification.

Conditioned media containing EphA4-Fc (10–15 L) was concentrated 10-fold using tangential flow filtration (Centramate, Pall Corporation, USA) with a 900 sq cm, polyether sulfone membrane (Pall Corporation, USA) as per the manufacturer's instructions. The conditioned media was dialyzed into phosphate-buffered saline (PBS) post concentration.

The concentrated conditioned media was applied to a 10 mL Protein A affinity chromatography column (mAb select, GE, Sweden) by gravity feed, and washed with 250 mL PBS. Bound EphA4-Fc was eluted with 0.1M citrate buffer (pH 3.0) and 10 mL fractions were neutralized with 2 mL 2M Tris buffer (pH 8.0).

Fractions were loaded onto an ion exchange resin (HiLoad Q 26/10, GE, Sweden) using an AKTA explorer High-performance liquid chromatography (HPLC) at a flow rate of 10 mL/min with a 30 min linear gradient between Tris buffer (20mM pH 8) and Tris buffer containing sodium chloride (2M). Absorbance at 280 nm was used to monitor and collect peak fractions.

Size exclusion was used to separate the dimeric EphA4-Fc protein from other molecular weight species. Typically a Superdex 200 (47/50) column was used to purify the EphA4-Fc protein in PBS containing azide. Fractions were selected based on the observation of a single species in an analytical size exclusion column (Superose 200 3.2/30). Samples were subsequently dialyzed into mouse tonicity (MT)-PBS using a 30 mL cassette slidalyzer. (Thermo Fisher Scientific Inc., USA).

The final pool of EphA4-Fc was generated after final quantitation and endotoxin testing. Endotoxin levels were quantitated using a lipopolysaccharides (LPS) kit based on Pylchome chromogenic endotoxin assay (Associates of Cape Code Inc., USA) as per manufacturer's instructions. Protein quantitation was calculated based on 1.0 absorbance unit at 280 being equivalent to 1.3 mg/mL. Purity was based on sodium dodecyl sulfate polyacrylamide gel electrophoresis (SDS-PAGE) and proteins visualized by coomassie stain. Binding properties of the recombinant proteins were confirmed using real time surface plasmon resonance analysis as described previously.^{27,28}

Western analysis of EphA4 blocking and activation

The cDNA encoding mouse EphA4 (nucleotides 55–3024; NM_007936.3) was cloned into the expression vector pEF-BOS²⁹ and transfected into Chinese hamster ovary (CHO) cells. A stably expressing EphA4 clonal line was generated and grown in humidified 5% CO₂ at 37°C in Dulbecco's Modified Eagle Medium (DMEM)/F12 media supplemented with 10% fetal bovine serum, penicillin (100 U/mL) and streptomycin (100 μg/mL). For EphA4 activation assays ($n=3$), 80–90% confluent cultures were serum starved for 2 h. EphA4-Fc was added at 2, 5, or 10 μg/mL 30 min before ephrin A4-Fc was added at 1 μg/mL. After 30 min activation with ephrin A4-Fc, cells were lysed in radio immunoprecipitation assay (RIPA) buffer (150 mM sodium chloride, 1% Triton X-100, 0.5% sodium deoxycholate, 0.1% sodium dodecyl sulphate, 50 mM Tris, pH 8) with sodium orthovanadate (1 mM), phenylmethane-sulfonyl fluoride (1 mM) and Complete Protease Inhibitor Cocktail (1×; Roche Applied Science). Lysates were clarified by centrifugation at 14,000 relative centrifugal force (rcf) for 10 min at 4°C, and an estimate of the protein concentration was determined using a bicinchoninic acid assay (Pierce Biotechnology, Inc.). Reduced protein (50 μg) was separated by electrophoresis (4–12% SDS-PAGE, Novex® NuPage®, Invitrogen) and transferred onto Immobilon FL membrane (Millipore). Membranes were blocked with 5% skim milk powder in phosphate-buffered saline, 0.02% Tween 20 (PBST) for 1 h. Primary antibodies (mouse anti-EphA4, ECM Biosciences; rabbit anti-phosphoTyr602-EphA4, ECM Biosciences) were allowed to bind overnight in 5% skim milk powder in PBST at 4°C. After washing with PBST, bound antibodies were detected using IRDye® secondary reagents (Li-COR Biosciences) and bands were detected using the Odyssey system (Li-COR Biosciences). Absolute integrated intensity values were extracted and adjusted for background values, and the intensity of phosphorylated EphA4 was normalized to total EphA4 levels. Relative values were expressed as a percentage of the mean untreated value.

Surgical procedures

All animals were treated in accordance with the Australian Code of Practice for the Care and Use of Animals for Scientific Purposes, and ethical approval was obtained from the University of Queensland Anatomical Biosciences Ethics Committee.

Adult female Wistar rats (10–12 weeks old, 200–250 g) were housed in groups of two or three animals and maintained on a 12 h light:12 h dark cycle with *ad libitum* access to food and water. Prior to surgery, animals were acclimated to handling and the experimental environments for 2 weeks. Rats were anesthetized with a combination of ketamine and xylazine (100 mg/kg and 10 mg/kg, respectively). An incision was made through the skin and muscles overlying the thoracic spine to expose the T9–T11 vertebrae. The spinal cord (approximate spinal level T11/12) was exposed by a dorsal laminectomy at T10. The spine was then immobilized using two Adson forceps, placed at T9 and T11, respectively. A force-defined contusive injury of 150 kdynes was inflicted using the Infinite Horizons impactor device.³⁰ Following impact, the musculature and skin were closed in separate layers with sutures, after which the animals were returned to their home cage to recover. Experimental rats were treated with antibiotics (Baytril, 2 mg/kg) and pain relief (Torbugesic, 2 mg/kg) for 48 h. Bladders were manually expressed twice daily for up to 2 weeks, or until bladder control was recovered. One animal receiving treatment with 5 mg/kg EphA4-Fc died just prior to perfusion. Postmortem examination did not reveal any specific cause of death related to the SCI or treatment. As such, we included its behavioral data for analysis, but could not include it for MRI or DTI analysis.

EphA4-Fc delivery

Animals were randomized prior to recovery from anesthesia and given their first treatment 2 h after surgery. All treatments were delivered by intraperitoneal injection. Animals received initial doses of 40 mg ($n=11$), 10 mg ($n=12$) or 2 mg ($n=10$) EphA4-Fc per kg body weight, whereas controls received injectable saline as the vehicle ($n=12$). Animals then received additional EphA4-Fc or saline injections at half the original dose (i.e., 20 mg, 5 mg, or 1 mg per kg body weight) every second day from 24 h post-injury up to 14 days post-injury (DPI). Researchers involved in assessing injury outcomes were blinded to the treatment.

Circulating EphA4-Fc in sera detected by enzyme-linked immunosorbent assay (ELISA)

Serum levels of circulating EphA4-Fc were measured on days 7, 14, and 21 after injury by sandwich ELISA. Briefly, 200–300 μ L of blood was collected from the tail and allowed to clot for 30 min at room temperature. Serum was separated by centrifugation at 1500g for 10 min and stored at -80°C prior to analysis. High-capacity binding ELISA plates (Greiner) were coated with a monoclonal antibody targeting the extracellular domain of EphA4 and blocked with 1% bovine serum albumin. Triplicate samples of diluted serum were applied to the plates and the presence of the recombinant EphA4-Fc was detected using a horseradish peroxidase (HRP)-conjugated goat anti-human IgG Fc polyclonal antibody and the SigmaFAST[®] o-phenylenediamine dihydrochloride (OPD) substrate (Sigma Aldrich). A standard curve was generated using purified EphA4-Fc at concentrations between 0 and 200 ng/mL.

Ledged tapered balance beam task

This task requires rats to cross an elevated, tapered (6.5–2.5 cm) beam, 1.4 m in length, with support ledges on either side at a height 2 cm lower than the upper surface of the beam. Rats were trained to cross the beam (four trials per day) on the 2 days immediately prior to testing at 120 days after injury, that is, the end of the experiment period. The distance to first misstep, where the animal failed to step on the upper surface, and the total number of substantial missteps (i.e., where the animal failed to straddle the beam or fell from the beam) over four trials were recorded and averaged. This assay provides a quantitative measure of functional deficits, specifically in relation to skilled paw placement, coordination, and balance of impaired rats.^{31,32}

Open-field locomotor performance

We assessed and scored open-field locomotor ability according to the 21 point Basso, Beattie and Bresnahan (BBB) locomotor rating scale.³³ This nonlinear scale was developed to discriminate between functional outcomes following SCI in rats. It is broken up into three divisions, with scores of 0–7 describing joint and limb movement, 8–14 describing weight-supported stepping and forelimb–hindlimb coordination, and 15–21 describing finer aspects of locomotion that include toe clearance and paw rotation.³³ Animals were assessed twice a week for the first fortnight, once a week for the next 6 weeks, and once at the end of the experiment (120 DPI). Scoring was performed over a 4 min period by two blinded assessors; the average score for each animal was used for statistical analysis.

MRI

Following the final behavioral tests at 120 days after injury, rats were deeply anesthetized with an overdose of sodium pentobarbital (300 mg/kg; Virbac), before being transcatheterially perfused with cold PBS followed by 4% paraformaldehyde in PBS. The vertebral column was dissected and post-fixed in 4% paraformaldehyde in PBS for 48 h at 4°C . For *ex vivo* MRI scans, vertebral columns were extensively washed in PBS and subsequently placed in a 0.2% solution of Magnevist[®] (gadopentetate dimeglumine; Bayer Healthcare) for at least 48 h, to enhance contrast between gray and white matter. Samples were next immersed in perfluorocarbon solution (Fomblin Y06/06, Solvay Solexis, Italy) for imaging. We examined six to eight animals from each treatment group by conventional high-resolution MRI; additional DTI analysis was performed for rats from the vehicle, 5 mg/kg EphA4-Fc, and 20 mg/kg EphA4-Fc treatment groups. Three 24-week-old uninjured controls were examined in an identical fashion for both MRI and DTI to obtain baseline measures.

MRI was performed using a Bruker 16.4T small animal MR imaging system, with a vertical wide bore that was equipped with a Micro2.5 gradient set (Karlsruhe, Germany; M2M Imaging, Australia) and 15 mm linear saw coil (M2M Imaging). High-resolution imaging was performed using Bruker gradient echo fast low angle shot magnetic resonance imaging (FLASH) sequence with TR/TE = 40/7.5 ms, 25 degree flip angle, four excitations and, 50 kHz spectral width. Images were acquired with a $28 \times 12.8 \times 12.8$ mm field-of-view with $560 \times 420 \times 420$ matrix to produce a 30×30 μ m coronal plane and 50 μ m slice resolution.

Following the conclusion of high-resolution MRI, spinal cords were dissected from the vertebral column. DTI was performed on the 16.4T MR system using a 10 mm Quadrature coil (M2M Imaging), with the following DTI-spin echo imaging parameters: TR/TE = 400/24 ms, $\delta/\Delta = 2/15$ ms, 2 excitations, 6 non-collinear diffusion encoding directions ([1,1,0],[1,0,1],[0,1,1],[-1,1,0],[1,0,-1],[0,-1,1]) and 1 B0 image. Images were acquired using a $22.3 \times 5 \times 5$ mm field-of-view with a $420 \times 96 \times 96$ matrix to give 50 μ m three dimensional (3D) isotropic resolution.

MRI and DTI analysis

Each region of interest (ROI) corresponding to the dorsal funiculus, gray matter, ventrolateral white matter, damaged tissue (atypical appearance compared to normal, uninjured tissue), and cystic cavitation was outlined using the closed polygon ROI tool in Osirix v3.9.2³⁴ or ImageJ in coronal slices that were spaced 0.5 mm apart over a 10 mm segment of the spinal cord. For uninjured animals, ROIs were examined every 1 mm over the same distance. For injured animals, the coronal slice that showed the smallest cross-sectional area of the spinal cord was defined as the epicenter. In all cases, this was located within 1 mm of the junction of the T9 and T10 vertebral bodies. The 10 mm field of view covered at least two vertebral levels containing the full extent of the cystic cavity and the vast majority of

observable pathology. The areas for each region were extracted for statistical evaluation and graphical analysis.

For DTI analysis, data reconstruction and fiber tracking were performed using Diffusion Tracker v0.6.0.1.³⁵ The default 25 degree angle threshold was increased to 35 degrees. This angle threshold allowed tracking up to 35 degrees and facilitated tracking at and near the injury epicenter. Ordered eigenvalue tensor parameters (λ_1 , λ_2 , and λ_3) were determined. The output from Diffusion Tracker was then imported into TrackVis v0.5.1.³⁵ The selection of coronal slices paralleled the MRI analysis. For DTI, ROIs corresponding to the dorsal funiculus were manually outlined from the diffusion weighted image every 0.5 mm over 10 mm (including uninjured animals), centered at the epicenter (least cross-sectional area). Where the dorsal column was not easily identifiable because of tissue damage, tracks to show connectivity between ROIs were generated from rostral or caudal ROIs to aid selection. For each ROI, cross-sectional area and mean values of apparent diffusion coefficient (ADC), axial diffusivity, radial diffusivity, and fractional anisotropy (FA) were extracted. Diffusion along the principal axis of the diffusion ellipsoid was defined as axial diffusivity ($D_{||} = \lambda_1$) and radial diffusivity as the average of the two minor eigenvalues [$D_{\perp} = (\lambda_2 + \lambda_3)/2$]. To quantify the degree of anisotropic diffusion, fractional anisotropy was calculated $\{FA = \sqrt{1/2}[\sqrt{(\lambda_1 - \lambda_2)^2 + (\lambda_1 - \lambda_3)^2 + (\lambda_2 - \lambda_3)^2}]/\sqrt{[\lambda_1^2 + \lambda_2^2 + \lambda_3^2]}\}$. A FA value of 0 indicates complete isotropic diffusion and a value of 1 indicates diffusion in one direction only (complete anisotropy).

Sensory testing

Spinal reflex sensitivity in SCI rats was determined using the Randall–Selitto deep pressure assay³⁶ and the von Frey assay² at 120 days following the injury. The Randall–Selitto and von Frey tests were conducted on different days. Each assay was performed in triplicate on both the left and right hindpaws, with 10–15 min between individual measurements; the values were then averaged. For the Randall–Selitto test (Analgesy meter LE7306, Harvard Apparatus), rats were gently restrained by hand and the maximum

tolerated pressure on the pad of the hindlimb (3 mm diameter blunt tip) that caused either a voluntary withdrawal reflex of the hindlimb or vocalization was defined as the pain threshold. Sensitivity to punctate stimulation was determined in the same manner using an electronic von Frey apparatus (EVF3, Bioseb Instruments).

Statistical analysis

Results are expressed as arithmetic mean \pm standard error of the mean (SEM). Data sets were examined for statistically significant differences between treatment groups using standard tests incorporated in GraphPad Prism v5.0. Analyses included unpaired *t* test for direct comparisons between two groups, one way and two way ANOVAs for multiple groups, and longitudinal analyses with appropriate post-hoc testing. Significance for specific locomotor outcomes in the open-field assay (BBB) and ledged balance beam assay were determined using receiver-operator characteristic (ROC) curve analysis and tested by Fisher's exact test. A $p < 0.05$ was considered significant for all statistical analyses.

Results

Soluble EphA4-Fc prevents ephrin-induced activation of EphA4

To verify that EphA4-Fc could block ephrin-dependent EphA4 activation, we compared phosphorylation levels of EphA4 following treatment with 1) ephrin A4-Fc, 2) EphA4-Fc, and 3) ephrin A4-Fc and EphA4-Fc. We showed that 1 $\mu\text{g}/\text{mL}$ ephrin A4-Fc activated EphA4 and caused a significant increase in EphA4 phosphorylation, and that the addition of EphA4-Fc effectively blocked ephrin-dependent phosphorylation ($p < 0.001$; Fig. 1A, B). Importantly, blocking of EphA4 activation was achieved at concentrations of EphA4-Fc similar to that detected in rat serum following treatment with 5 mg/kg and 20 mg/kg EphA4-Fc. Two

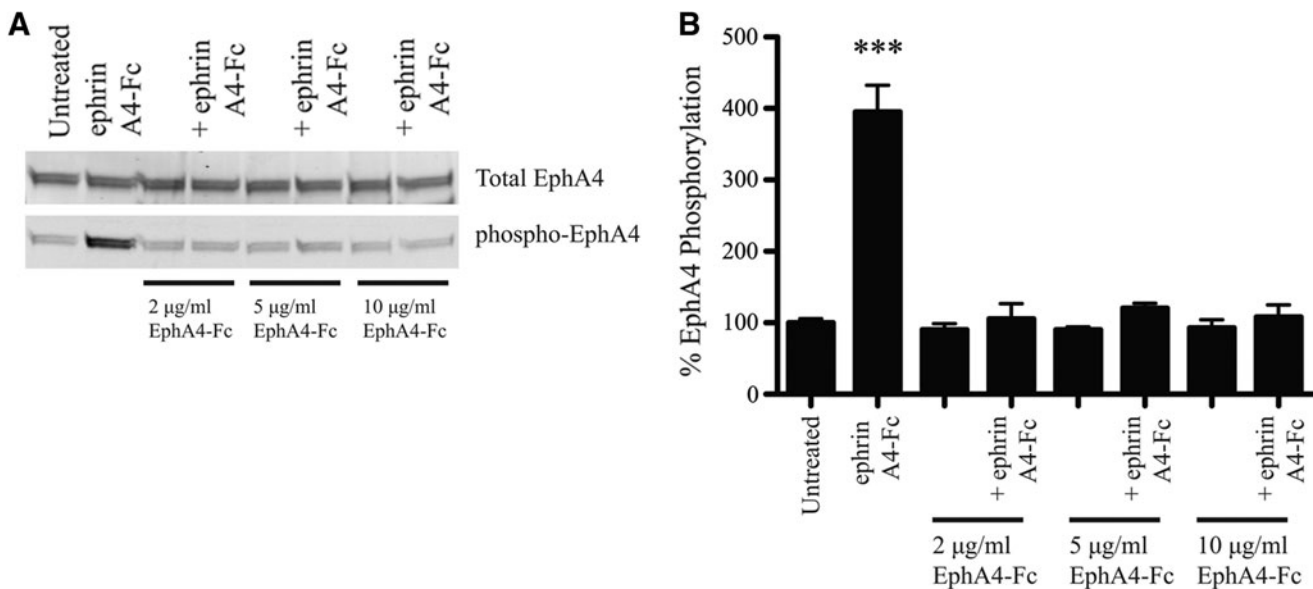


FIG. 1. EphA4-Fc prevents ephrin-induced phosphorylation of EphA4. (A) Chinese hamster ovary (CHO) cells expressing EphA4 were blocked with EphA4-Fc prior to the addition of ephrin A4-Fc. Lysates were separated by sodium dodecyl sulfate polyacrylamide gel electrophoresis (SDS-PAGE) and bands specific for total EphA4 and phosphorylated EphA4 detected. (B) Quantification of band densities shows that only in the absence of EphA4-Fc could ephrin A4-Fc significantly increase the phosphorylation of EphA4 above basal levels (one-way ANOVA with Bonferroni's post-test). Blocking with EphA4-Fc prevented ephrin-induced phosphorylation of EphA4. *** $p < 0.001$.

weeks following SCI, the circulating levels of EphA4-Fc were recorded to be $3.5 \pm 1.1 \mu\text{g/mL}$ and $24 \pm 3.9 \mu\text{g/mL}$ for the 5 mg/kg and 20 mg/kg groups, respectively. EphA4-Fc was not detected above background levels in rats treated with 1 mg/kg EphA4-Fc.

To check that the naïve rat did not generate an immune response to the EphA4-Fc fusion protein, EphA4-Fc-treated rats were examined for the presence of rat antibodies that targeted EphA4-Fc. One rat (from the 1 mg/kg treatment group) showed an immune response and performed extremely poorly in the balance beam task. This rat was excluded from all tests measuring locomotor performance.

EphA4-Fc improved functional outcome following contusive SCI

We have previously shown, using a mouse model of lateral hemisection SCI, that administration of EphA4-Fc at 20 mg/kg promoted functional recovery and axonal regrowth.¹⁸ Although the lesion model is useful for studying regeneration, it has limited relevance to the majority of human SCI cases. To assess the effectiveness of EphA4-Fc treatment in the present study, we used a rat model of contusive SCI, as it replicates many of the pathological features seen in human SCI cases.

We used the ledged tapered beam assay to obtain a quantitative measure of skilled limb placement. This assay interrogates aspects of balance and coordination of rats as they cross a narrowing, raised beam, and has been previously used to measure functional differences following SCI.^{31,37} At 120 days following the injury, we observed a dose-dependent improvement in rats treated with EphA4-Fc (Fig. 2A). Rats treated with 5 mg/kg and 20 mg/kg traversed 106 ± 7.5 cm and 118 ± 5.7 cm, respectively, of the 140 cm ledged tapered beam without error, as compared with the vehicle-treated group, which averaged only 76.4 ± 11.3 cm. Although rats treated with 1 mg/kg EphA4-Fc did not differ significantly from the vehicle-treated group in the distance traveled until first misstep (94 ± 10.7 cm; Fig. 2A), they recorded significantly fewer falls or serious missteps compared with the vehicle-treated group

($p < 0.05$; Fig. 2B). When the data from all treated rats were pooled, an overall positive effect of EphA4 blocking was observed. EphA4-Fc-treated rats were able to cross a significantly greater distance of the beam without error than were rats treated with the vehicle alone ($p < 0.01$; Figure 2C). Response to EphA4-Fc treatment was also assessed using a second means, namely an ROC. Using this model, we determined 100 cm to be the threshold at which a positive response to treatment could be recorded. If animals crossed less than this distance before first misstep, a negative response to treatment was recorded. Of the animals that received EphA4-Fc, 64% (21/33) recorded a positive response, compared with only 25% (3/12) of vehicle-treated animals. Overall, using this method of analysis, EphA4-Fc-treated animals performed significantly better than vehicle-treated rats on the ledged balance beam ($p = 0.0406$, Fisher's exact test).

At 120 DPI, we assessed the performance of EphA4-Fc-treated and vehicle-treated rats in the open field using the BBB locomotor rating scale (Fig. 3). All treated groups showed mean BBB scores higher than that of the control group; however, because of the size and variation within the groups, this improvement was only statistically significant for rats treated with 1 mg/kg EphA4-Fc ($p < 0.01$; Fig. 3A). When data from all EphA4-treated rats were pooled and compared with controls, at 120 days following injury, a significant improvement in functional recovery was observed ($p < 0.05$; Fig. 3B). Using ROC curve analysis, a BBB score > 12 (correlating to occasional coordination and weight-supported plantar stepping or better) was determined as the minimum score for a positive response to treatment. A significantly greater number of EphA4-Fc treated rats (91%, 30/33) recorded a positive result to treatment when compared with the vehicle-treated rats (58%, 7/12) ($p = 0.0224$, Fisher's exact test).

MRI and DTI showed structural improvement following treatment with EphA4-Fc after SCI

Next, at 120 days following injury, MRI and DTI data were collected and used to assess whether EphA4-Fc had any positive

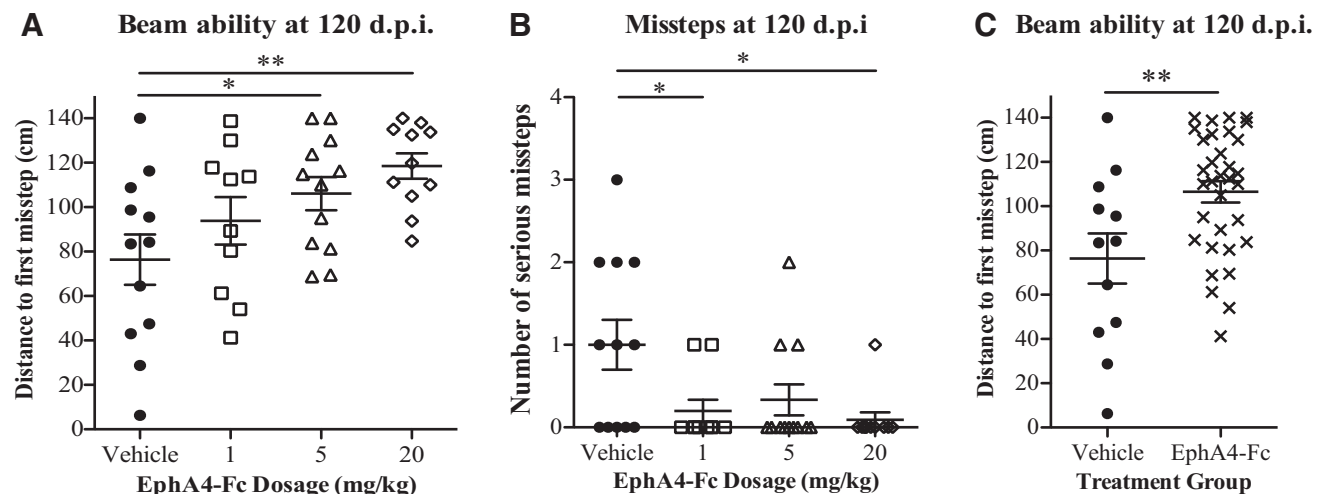


FIG. 2. EphA4-Fc improves coordination and balance after contusive spinal cord injury (SCI). **(A)** At 120 days following injury, animals treated with 5 mg/kg or 20 mg/kg EphA4-Fc showed a significant improvement in their ability to cross the ledged, tapered beam before misstepping (one-way ANOVA with Dunnett's post-test). **(B)** Rats treated with 1 mg/kg or 20 mg/kg EphA4-Fc had significantly fewer falls than animals treated with the vehicle (one way ANOVA with Dunnett's post test; $p = 0.074$ for animals treated with 5 mg/kg EphA4-Fc, unpaired t test). **(C)** When data from all EphA4-Fc treatment groups were pooled, the mean distance before a misstep for animals treated with EphA4-Fc was significantly greater than for animals treated with vehicle alone (unpaired t test). * $p < 0.05$, ** $p < 0.01$; d.p.i.: days post-injury.

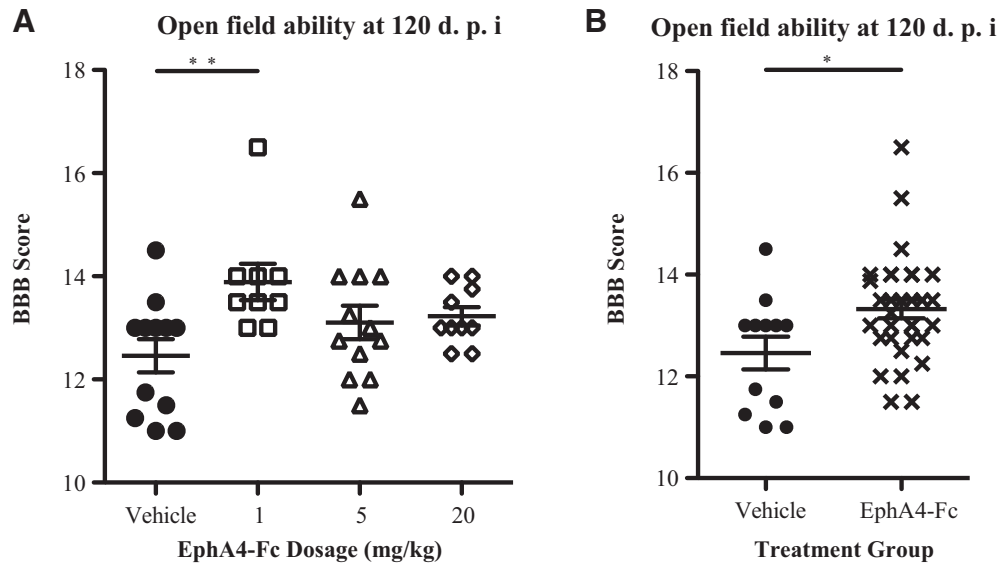


FIG. 3. EphA4-Fc improves open-field locomotor performance after contusive spinal cord injury (SCI). **(A)** At 120 days following injury, rats treated with 1 mg/kg EphA4-Fc had significantly better Basso, Beattie and Bresnahan (BBB) scores than rats treated with the vehicle alone (one-way ANOVA with Dunnett's post-test). **(B)** When combined, all EphA4-Fc treated animals had significantly better open-field locomotor performance than did controls (unpaired *t* test). **p* < 0.05, ***p* < 0.01; d.p.i.: days post-injury.

structural effect on the injured spinal cord. As the images obtained were of very high resolution, it was possible to accurately discriminate between different regions of the cord (termed ROIs) and between normal and damaged tissue. Representative examples of mid-sagittal views of MRI scans are shown in Figure 4A–D, and an example of a coronal slice (from Fig. 4B) is shown in Figure 4E and F.

Overall, we found no significant treatment effect when comparing the area of normal tissue at the epicenter in spinal cords from vehicle- ($42.0 \pm 5.4\%$, $n=7$) and EphA4-Fc-treated rats ($31.9 \pm 4.8\%$: 1 mg/kg [$n=7$]; $43.0 \pm 4.8\%$: 5 mg/kg [$n=6$]; $43.4 \pm 9.8\%$: 20 mg/kg [$n=8$]). To examine the structure of the spinal cord more closely, we quantified the area within each of the five ROIs, namely the dorsal funiculus, gray matter, ventrolateral white matter, cysts, and damaged tissue (Fig. 4). Compared with controls, we observed a significant increase in the cross-sectional area of the dorsal funiculus caudal to the lesion epicenter in EphA4-Fc treated animals ($p < 0.05$ at 2.5 mm for the 1 mg/kg group; $p < 0.05$ at 1.5 and 2.0 mm and $p < 0.01$ at 2.5 mm for the 5 mg/kg group; $p < 0.05$ at 3.0 mm for the 20 mg/kg group; Fig. 4G–J). No significant difference in cross-sectional area was observed for the remaining ROIs; however, 60% (12/20) of the EphA4-Fc-treated rats had ventrolateral white matter with a greater cross-sectional area than the maximum cross-sectional area recorded for all vehicle-treated rats (Supplementary Fig. 1) (see online supplementary material at <http://www.liebertpub.com>). Overall, the mean area of the ventrolateral white matter was $1.12 \pm 0.06 \text{ mm}^2$ for the EphA4-Fc group and $0.92 \pm 0.11 \text{ mm}^2$ for vehicle-treated rats. Although not significant, these data suggest a trend toward improved structural integrity following treatment.

Using DTI, we examined spinal cords from the 5 mg/kg ($n=8$) and 20 mg/kg ($n=6$) treatment groups, as these groups showed the most significant treatment response, and compared them with those treated with vehicle alone ($n=7$). An example of mid-sagittal views of DTI images, with ROIs highlighted, are shown in Figure 5A–D. We found that the DTI data confirmed our MRI analysis, as the area

of the dorsal funiculus caudal to the injury site was larger in animals treated with EphA4-Fc (Fig. 5E). As expected after contusive SCI, in all animals, that is, both EphA4-Fc- and vehicle treated, a decrease in fractional anisotropy was observed throughout the injury site (Fig. 5F) and increases in ADC and axial and transverse diffusivity were observed at the center of the lesion (Fig. 5G–I).

EphA4-Fc had acute effects on locomotor performance after contusive SCI

Our observations that rats treated with EphA4-Fc had improved locomotion and increased cross-sectional area of the dorsal funiculus may indicate preservation of white matter. To assess this possibility, we analyzed the open-field performance of the injured rats in the acute phase – 1, 3, and 14 days – following SCI, and found that the 1 mg/kg and 5 mg/kg treatment groups performed significantly better than the control group at all three time points ($p < 0.05$ for 1 mg/kg and $p < 0.01$ for 5 mg/kg at 1 DPI; $p < 0.01$ for 1 mg/kg and $p < 0.05$ for 5 mg/kg at 3 DPI; $p < 0.01$ for 1 mg/kg and $p < 0.05$ for 5 mg/kg at 14 DPI; one-way ANOVA; Fig. 6A–C). These improvements suggest that EphA4-Fc has positive effects in the acute period after contusive SCI possibly because of preservation, although the exact mechanism is yet to be elucidated.

EphA4-Fc did not increase nociceptive sensitivity

It has previously been reported that small interfering RNA (siRNA)-mediated downregulation of EphA4 expression increased the sensitivity of animals to nociceptive pain following SCI.³⁸ To test for sensory hypersensitivity after EphA4-Fc treatment, we used the electronic von Frey point stimulation assay (Fig. 7A) and the Randall–Selitto broad pressure assay (Fig. 7B). Uninjured animals showed a mean nociceptive response to a force of 22.63 g ($\pm 0.55 \text{ g SEM}$; $n=2$) in the von Frey assay and 313.6 g ($\pm 42.63 \text{ g SEM}$; $n=2$) for the Randall–Sellito assay. Slightly increased sensitivity in von Frey thresholds was observed as a result of SCI, which was independent of treatment; however, none of the treatment groups

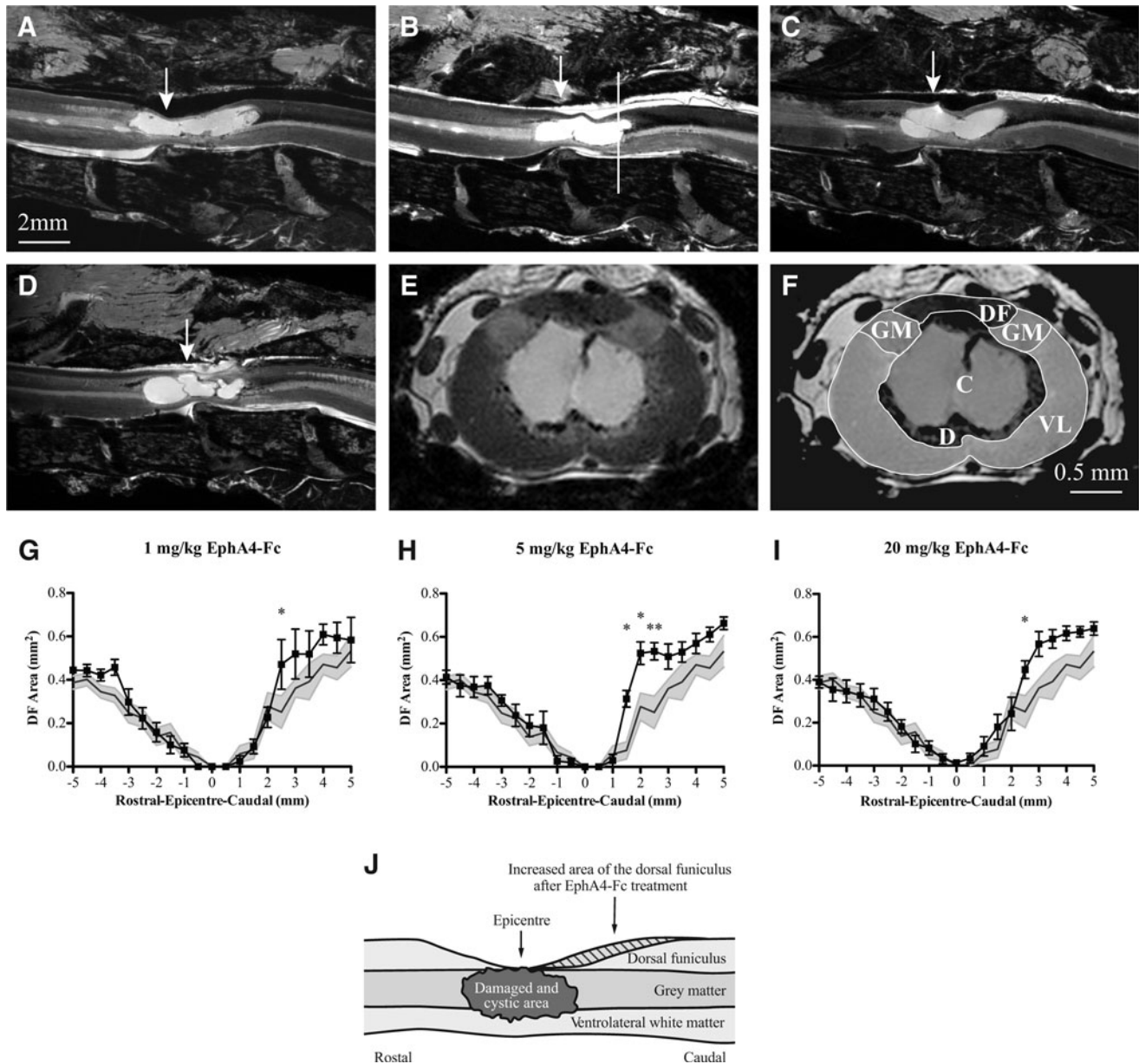


FIG. 4. MRI analysis shows that the area of the dorsal funiculus is greater following EphA4-Fc treatment after spinal cord injury (SCI). Examples of high-resolution MRI mid-sagittal views of injured spinal cords from rats treated with (A) vehicle alone ($n=7$), (B) 1 mg/kg ($n=7$), (C) 5 mg/kg ($n=6$), and (D) 20 mg/kg EphA4-Fc ($n=8$). (E) Example of a coronal MRI slice (from [B], white line indicates location), with regions of interest (ROIs) shown in (F). DF: dorsal funiculus; GM: gray matter; VL: ventrolateral white matter; C: cyst; and D: damaged tissue. (G–I) The area of the dorsal funiculus in rats treated with (G) 1 mg/kg, (H) 5 mg/kg, and (I) 20 mg/kg EphA4-Fc was significantly greater caudal to the injury epicenter when compared with controls. The area of the dorsal funiculus for rats treated with the vehicle is shaded to the extent of its standard error of the mean. (J) A schematic of the increased area of the dorsal funiculus caudal to the injury epicenter (striped area) in EphA4-Fc-treated rats compared with rats treated with the vehicle alone. Scale bars for panels (A–D) as indicated in (A), and for (E) and (F) as indicated in (F). * $p < 0.05$, ** $p < 0.01$, two-way ANOVA with Bonferroni's post-test.

differed significantly in their response to the point stimulation assay when compared with vehicle-treated controls (Fig. 7A). In the Randall–Selitto test, animals treated with 5 mg/kg or 20 mg/kg of EphA4-Fc were less sensitive than vehicle-treated animals to the broad pressure assay (Fig. 7B), however, their responses were not significantly different to responses from uninjured animals. As such, we found no evidence of increased nociceptive sensitivity in EphA4-Fc-treated animals.

Discussion

In the current study, we assessed the efficacy of EphA4-Fc therapy in a contusion injury model that more accurately mimics the pathology associated with the majority of human SCI cases. Here, we observed significant improvements in the functional outcomes and identified anatomical changes in the spinal cords of EphA4-Fc-treated rats compared with vehicle-treated rats.

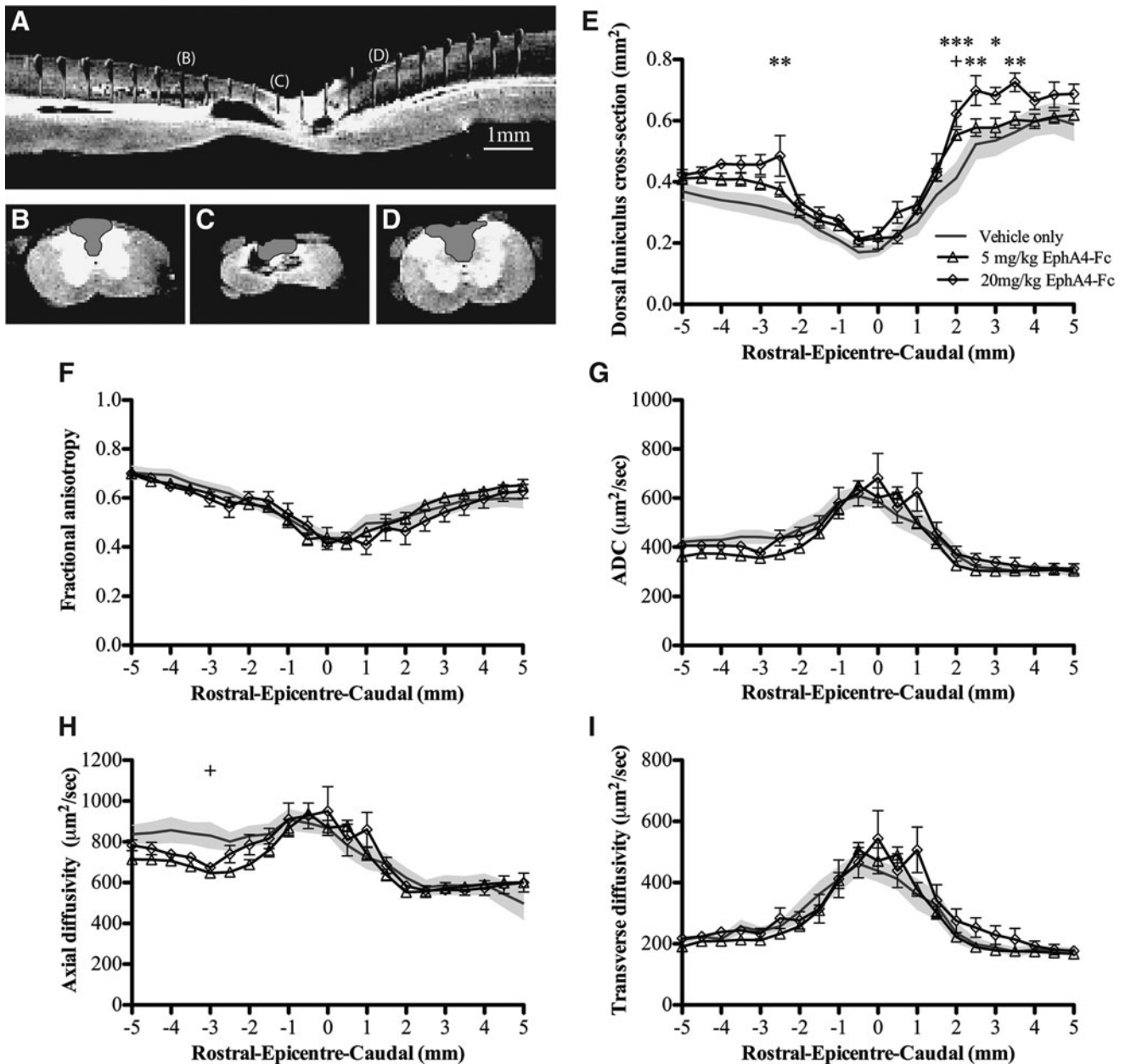


FIG. 5. Diffusion tensor imaging (DTI) analysis shows that the area of the dorsal funiculus is greater following EphA4-Fc treatment after spinal cord injury (SCI). (A–D) Example of a high-resolution DTI midsagittal images. Examples of the regions of interest (ROIs) from (A) are shown in (B–D) (rostral to caudal, B: -2.0 mm, C: 0.0 mm, D: +2.0 mm). (E) The cross-sectional area of the dorsal funiculus in the 5 mg/kg group was significantly greater 2 mm caudal to the injury epicenter, and in the 20 mg/kg EphA4-Fc treatment group, the area was significantly greater 3 mm rostral and 2–3.5 mm caudal to the lesion epicenter. Quantitative measures of diffusion (F, fractional anisotropy; G, apparent diffusion coefficient; H, axial diffusivity; and I, transverse diffusivity) reveal an increasing loss of white matter integrity closer to the lesion epicenter. The vehicle-treated group is shaded to the extent of its standard error of the mean. Scale bar for (A–D) as indicated in (A). + $p < 0.05$, * $p < 0.05$, ** $p < 0.01$, *** $p < 0.001$, two-way ANOVA with Bonferroni's post-test.

Therapeutic targeting of members of the Eph:ephrin system has been suggested to have great clinical value. Ephrin-A1-Fc, injected after myocardial infarction, has shown efficacy in reducing tissue damage in mice,³⁹ whereas EphA2-Fc reduced tumor burden in a pancreatic ductal adenocarcinoma model in mice.⁴⁰ We recently reported that recombinant protein antagonists of EphA4 (ephrin-A5-Fc and EphA4-Fc) improved outcomes in a lateral hemisection model of SCI in mice,¹⁸ mirroring the positive effects that were observed following genetic deletion of EphA4.¹⁷ These findings

were accompanied by the observation that mice treated with EphA4-Fc or ephrin-A5-Fc after SCI showed evidence of axonal regeneration in the lateral white matter and signs of decreased gliosis.¹⁸ We have also observed a positive response to treatment with the full-length EphA4-Fc compared with a deletion mutant of the recombinant EphA4-Fc protein, dLBD-EphA4-Fc, which lacked the key ligand-binding region (amino acids 20–274 of NP_031962.2). In a hemisection SCI model in wild-type C57 mice, we observed axonal regeneration through the lesion site in all

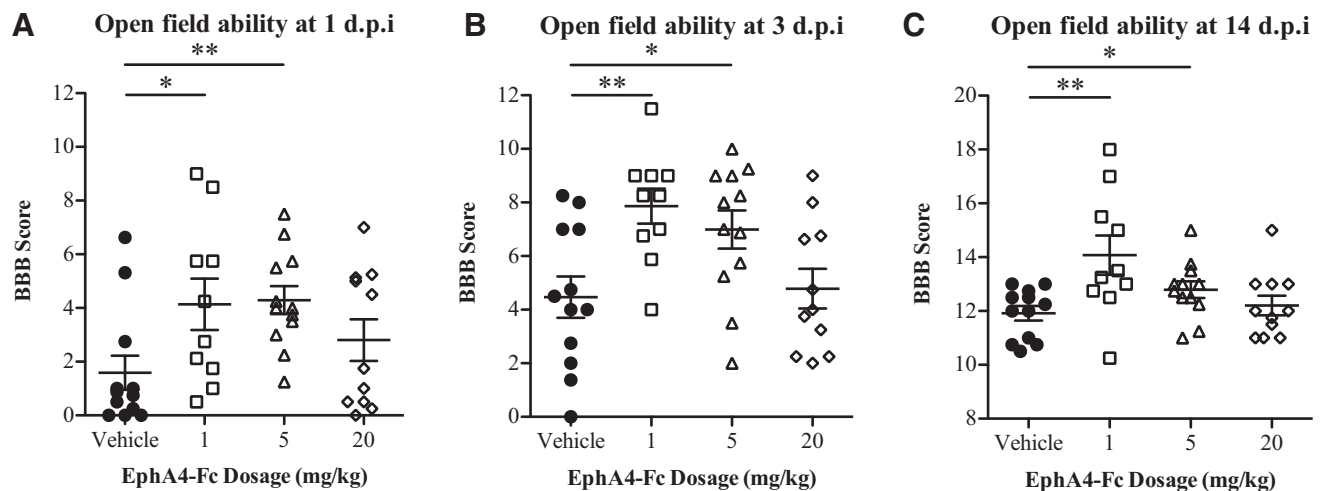


FIG. 6. EphA4-Fc treatment improves open-field locomotor performance in the acute phase after injury. When tested in the open field, rats treated with 1 mg/kg or 5 mg/kg EphA4-Fc had significantly higher Basso, Beattie and Bresnahan (BBB) scores than did vehicle-treated animals (A) 1 day, (B) 3 days, and (C) 14 days after contusive injury (one-way ANOVA with Dunnett's post-test). * $p < 0.05$, ** $p < 0.01$.

animals treated with the full-length protein, but saw no significant improvement in those treated with the mutated form (unpublished observation). Given this observation, and the fact that the human IgG4 has a significantly lower capacity to activate complement and a significantly lower ability to bind to the Fc gamma receptors, the probability of observing nonspecific Fc-mediated effects in our model was low.

Although *in vitro* data suggest that the major mechanism by which EphA4-Fc affects axon regeneration *in vivo* is primarily through modulation of the Rho-Rac-Cdc42 signaling cascades,^{17,41} the acute improvements presented here cannot be directly related to axon regeneration. We did not assess bulk axonal sparing/regeneration through anterograde tracing as, unlike the hemisection model of SCI,^{17,18} of the axons that traverse the injury site, there is no way to tell which were spared and which were severed by the original impact and subsequently regenerated. We therefore opted for more clinically relevant high-resolution MRI and DTI to assess

tissue integrity, and this assessment provided evidence of the therapeutic effect of EphA4-Fc administration in moderate contusive SCI.

Our current findings demonstrated that EphA4-Fc therapy resulted in a significant improvement in locomotor ability in rats with moderate contusive SCI. Modeling contusive injuries in rodents results in dorsally inflicted injuries and the resultant preservation in the ventrolateral quadrant of the spinal cord, which contains important tracts for general stepping and locomotion,^{42,43} makes the detection of improvement beyond the considerable degree of spontaneous recovery after SCI inherently more difficult. The BBB scoring system had limited capacity to identify improvements in locomotor ability following EphA4-Fc therapy after contusive SCI; however, the ledged tapered balance beam task, which assays for skilled paw placement, balance and coordination, revealed significant dose-dependent improvements in locomotor performance. The differences in sensitivity between these two tests is highlighted

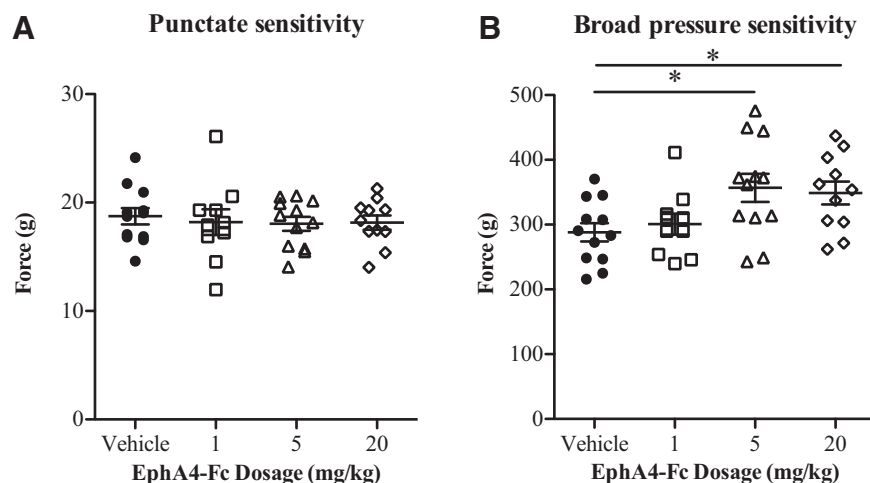


FIG. 7. EphA4-Fc treatment did not affect the nociceptive response to pressure. Treated animals did not show any increase in mechanical hyperalgesia as tested using the (A) von Frey assay and (B) the Randall-Siletto assay. The animals treated with 5 mg/kg or 20 mg/kg EphA4-Fc were significantly less sensitive using the Randall-Siletto measure of broad pressure pain (one-way ANOVA with Dunnett's post-test). * $p < 0.05$.

by the results of the 20 mg/kg EphA4-Fc treatment group, which showed increased area of the dorsal funiculus and significantly improved ability on the ledged tapered balance beam, but no significant improvement in open field ability as measured by BBB score.

Improvements in the locomotor ability of EphA4-Fc-treated rats suggest that EphA4-Fc treatment can improve SCI outcomes via mechanisms other than (or in addition to) restorative regrowth. A reduction in secondary injury, possibly as a result of a reduction in the severity of the inflammatory response, and resulting cellular damage and death, following EphA4-Fc treatment,⁴⁴ could explain the acute behavioral improvements observed, and may result in only small changes in the ventrolateral white matter detected at the epicenter by MRI.

It is also possible that EphA4-Fc improves synaptic function and/or plasticity. It has been shown that EphA4-positive neurons are a major component of the excitatory motor pathway that controls the central pattern generator for locomotion.¹¹ In conjunction with research that demonstrates that antagonism of EphA4 increases dendritic spine formation,⁴⁵ antagonizing Eph:ephrin activity within or distal to the lesion site may promote dendritic spinogenesis and synapse formation, thereby improving connectivity and function of the remaining ventrolateral white matter tracts, improving spontaneous locomotor ability as assessed by the open-field locomotor task. Our previous reports, however, suggest EphA4-Fc promotes functional improvements through axonal regeneration after contusive SCI,¹⁸ despite only a marginal decrease in astrogliosis. Therefore, it is more likely that EphA4 acts in a similar manner to what we described originally.¹⁰ More recent studies have shown that a lack of EphA4 promotes survival of motor neurons in the spinal cord of animals with experimental amyotrophic lateral sclerosis, indicating that blocking EphA4, in this case, may act to prevent cell death and preserve tissue after injury.⁴⁶ Given that the dorsal funiculus is required for voluntary or skilled locomotor ability,^{37,47} and our current observations of improved locomotion and larger dorsal funiculus after EphA4-Fc treatment, future studies will be needed to identify whether this improvement is caused by axon regeneration or preservation.

Although other studies have used MRI and DTI to examine SCI,^{24,48,49} this is the first reporting high-resolution data sets for MRI ($50\ \mu\text{m} \times 30\ \mu\text{m} \times 30\ \mu\text{m}$) and DTI ($50\ \mu\text{m} \times 50\ \mu\text{m} \times 50\ \mu\text{m}$) of contused rat spinal cords, and the first to use these measures to assess the effect of EphA4-Fc treatment. We observed a decrease in fractional anisotropy and an increase in diffusivity within the lesion, irrespective of directionality and/or treatment. This indicates that the white matter within the dorsal funiculus had lost structural and directional integrity. We also observed a significantly greater cross-sectional area of the dorsal funiculus through high-resolution MRI, particularly caudal to the site of injury in EphA4-Fc-treated groups. Our high-resolution DTI imaging analysis did not, however, reveal any clear evidence for greater structural tissue integrity in this area, and the biological significance of this observation remains undetermined. In contrast to our hypothesis that high-resolution DTI may detect changes caused by EphA4-Fc treatment, our results suggest that DTI after contusive SCI, even at high resolution, is unlikely to resolve differences in diffusion metrics of the spinal cord that result from therapeutic intervention. We conclude that MRI and DTI techniques, although useful for detecting gross anatomical differences (e.g., tissue sparing), are unlikely to detect small regenerative responses following therapeutic interventions in the corticospinal tract at current clinical resolutions, particularly as recent data suggest that the corticospinal tract does not undergo retrograde cell death and shows innate sprouting capability.^{50,51}

Induction of central pain syndromes resulting from the pathological sprouting and activation of astrocytes and microglia within the injured spinal cord (which sensitized the dorsal horn neurons to excitation through suppression of inhibitory synaptic activity), has been cited as a potential concern or side effect of regenerative therapies.^{52,53} In contrast to a previous study in which EphA4 was downregulated through siRNA-mediated knockdown,³⁸ we did not observe any behavior that indicated hypersensitivity in EphA4-Fc-treated rats using two different assessments of nociceptive sensitivity. In this case, siRNA repression of EphA4, as measured by semiquantitative polymerase chain reaction (PCR), was only partially successful, and would not prevent all the signaling interactions that can occur. In our case, EphA4-Fc acted as a promiscuous blocker of most Eph and ephrin interactions, and, as we present here, did not increase the sensitivity to nociceptive stimuli.

We have previously reported a significant reduction of astrocytic gliosis in EphA4 null mice following a hemisectional SCI,¹⁷ however, following the same type of injury, wild-type mice showed only a marginal reduction in gliosis when treated with EphA4-Fc or ephrin A5-Fc.¹⁸ We have recently published findings to suggest that the absence of a gliotic response in the EphA4^{-/-} mice following SCI may be the result of strain differences.⁵⁴ In addition, our MRI and DTI analyses only detected significant changes in normal white matter distal to the injury, and did not reveal any significant changes to lesion areas. As such, we concluded that the EphA4-Fc was unlikely to affect gliotic scarring, and in the event that it may have marginal effects, it is unlikely to be detected using MRI analysis.

Conclusion

In summary, the adult mammalian CNS has very limited ability to regenerate following disease or trauma, and the successful clinical intervention for SCI remains an elusive goal. Previous research has identified EphA4 as a key contributor to the lack of regenerative potential within the CNS. We show here that therapeutic antagonism of EphA4 with the recombinant protein antagonist, EphA4-Fc, provides functional benefits after a contusion injury in rats, and research is now required to elucidate the mechanisms through which EphA4-Fc may act. We have now shown the therapeutic effectiveness of EphA4-Fc in an animal model that shares many clinical features of human cases of SCI, and EphA4-Fc shows continued promise as a future therapeutic for spinal cord and possibly other neural injuries.

Acknowledgments

This work was supported by the National Health and Medical Research Council (Grants 511212 and APP1017308 to Prof. Bartlett) and the Australian Research Council (Grant DP110103201 to Prof. Bartlett). This work was also supported by funding from the Lisa Palmer bequest and Spinal Cure Australia. We acknowledge the assistance of Rowan Tweedale and Ashley Cooper (Queensland Brain Institute, The University of Queensland) for their critical review of this manuscript.

Author Disclosure Statement

No competing financial interests exist.

References

1. Liebscher, T., Schnell, L., Schnell, D., Scholl, J., Schneider, R., Gullo, M., Fouad, K., Mir, A., Rausch, M., Kindler, D., Hamers, F.P., and Schwab, M.E. (2005). Nogo-A antibody improves regeneration and locomotion of spinal cord-injured rats. *Ann. Neurol.* 58, 706–719.

2. Barritt, A.W., Davies, M., Marchand, F., Hartley, R., Grist, J., Yip, P., McMahon, S.B., and Bradbury, E.J. (2006). Chondroitinase ABC promotes sprouting of intact and injured spinal systems after spinal cord injury. *J. Neurosci.* 26, 10,856–10,867.
3. Hata, K., Fujitani, M., Yasuda, Y., Doya, H., Saito, T., Yamagishi, S., Mueller, B.K., and Yamashita, T. (2006). RGMa inhibition promotes axonal growth and recovery after spinal cord injury. *J. Cell Biol.* 173, 47–58.
4. Goldshmit, Y., McLenachan, S., and Turnley, A. (2006). Roles of Eph receptors and ephrins in the normal and damaged adult CNS. *Brain Res. Rev.* 52, 327–345.
5. Kaneko, S., Iwanami, A., Nakamura, M., Kishino, A., Kikuchi, K., Shibata, S., Okano, H.J., Ikegami, T., Moriya, A., Konishi, O., Nakayama, C., Kumagai, K., Kimura, T., Sato, Y., Goshima, Y., Taniguchi, M., Ito, M., He, Z., Toyama, Y., and Okano, H. (2006). A selective Sema3A inhibitor enhances regenerative responses and functional recovery of the injured spinal cord. *Nat. Med.* 12, 1380–1389.
6. Lau, E., and Margolis, R.U. (2010). Inhibitors of slit protein interactions with the heparan sulphate proteoglycan glypican-1: potential agents for the treatment of spinal cord injury. *Clin. Exp. Pharmacol. Physiol.* 37, 417–421.
7. Qin, H., Noberini, R., Huan, X., Shi, J., Pasquale, E.B., and Song, J. (2010). Structural characterization of the EphA4-Ephrin-B2 complex reveals new features enabling Eph-ephrin binding promiscuity. *J. Biol. Chem.* 285, 644–654.
8. Bowden, T.A., Aricescu, A.R., Nettleship, J.E., Siebold, C., Rahman-Hug, N., Owens, R.J., Stuart, D.I., and Jones, E.Y. (2009). Structural plasticity of eph receptor A4 facilitates cross-class ephrin signaling. *Structure* 17, 1386–1397.
9. Ho, S.K., Kovacevic, N., Henkelman, R.M., Boyd, A., Pawson, T., and Henderson, J.T. (2009). EphB2 and EphA4 receptors regulate formation of the principal inter-hemispheric tracts of the mammalian forebrain. *Neuroscience* 160, 784–795.
10. Dottori, M., Hartley, L., Galea, M., Paxinos, G., Polizzotto, M., Kilpatrick, T., Bartlett, P.F., Murphy, M., Kontgen, F., and Boyd, A.W. (1998). EphA4 (Sek1) receptor tyrosine kinase is required for the development of the corticospinal tract. *Proc. Natl. Acad. Sci. U.S.A.* 95, 13,248–13,253.
11. Kullander, K., Butt, S.J.B., Lebret, J.M., Lundfald, L., Restrepo, C.E., Rydstrom, A., Klein, R., and Kiehn, O. (2003). Role of EphA4 and EphrinB3 in local neuronal circuits that control walking. *Science* 299, 1889–1892.
12. Fabes, J., Anderson, P., Yanez-Munoz, R.J., Thrasher, A., Brennan, C., and Bolsover, S. (2006). Accumulation of the inhibitory receptor EphA4 may prevent regeneration of corticospinal tract axons following lesion. *Eur. J. Neurosci.* 23, 1721–1730.
13. Arocho, L.C., Figueroa, J.D., Torrado, A.I., Santiago, J.M., Vera, A.E., and Miranda, J.D. (2011). Expression profile and role of EphrinA1 ligand after spinal cord injury. *Cell. Mol. Neurobiol.* 31, 1057–1069.
14. Duffy, P., Wang, X., Siegel, C.S., Tu, N., Henkemeyer, M., Cafferty, W.B., and Strittmatter, S.M. (2012). Myelin-derived ephrinB3 restricts axonal regeneration and recovery after adult CNS injury. *Proc. Natl. Acad. Sci. U.S.A.* 109, 5063–5068.
15. Omoto, S., Ueno, M., Mochio, S., and Yamashita, T. (2011). Corticospinal tract fibers cross the ephrin-B3-negative part of the midline of the spinal cord after brain injury. *Neurosci. Res.* 69, 187–195.
16. Fabes, J., Anderson, P., Brennan, C., and Bolsover, S. (2007). Regeneration-enhancing effects of EphA4 blocking peptide following corticospinal tract injury in adult rat spinal cord. *Eur. J. Neurosci.* 26, 2496–2505.
17. Goldshmit, Y., Galea, M.P., Wise, G., Bartlett, P.F., and Turnley, A.M. (2004). Axonal regeneration and lack of astrocytic gliosis in EphA4-deficient mice. *J. Neurosci.* 24, 10,064–10,073.
18. Goldshmit, Y., Spanevello, M.D., Tajouri, S., Li, L., Rogers, F., Pearse, M., Galea, M., Bartlett, P.F., Boyd, A.W., and Turnley, A.M. (2011). EphA4 blockers promote axonal regeneration and functional recovery following spinal cord injury in mice. *PLoS ONE* 6, e24636.
19. Bilgen, M., and Rumboldt, Z. (2008). Neuronal and vascular biomarkers in syringomyelia: investigations using longitudinal MRI. *Biomark. Med.* 2, 113–124.
20. Bozzo, A., Marcoux, J., Radhakrishna, M., Pelletier, J., and Goulet, B. (2011). The role of magnetic resonance imaging in the management of acute spinal cord injury. *J. Neurotrauma* 28, 1401–1411.
21. Blomster, L.V., Cowin, G.J., Kurniawan, N.D., and Ruitenberg, M.J. (2013). Detection of endogenous iron deposits in the injured mouse spinal cord through high-resolution *ex vivo* and *in vivo* MRI. *NMR Biomed.* 26, 141–150.
22. Ellingson, B.M., Kurpad, S.N., and Schmit, B.D. (2008). *Ex vivo* diffusion tensor imaging and quantitative tractography of the rat spinal cord during long-term recovery from moderate spinal contusion. *J. Magn. Reson. Imaging* 28, 1068–1079.
23. Mac Donald, C.L., Dikranian, K., Song, S.K., Bayly, P.V., Holtzman, D.M., and Brody, D.L. (2007). Detection of traumatic axonal injury with diffusion tensor imaging in a mouse model of traumatic brain injury. *Exp. Neurol.* 205, 116–131.
24. Nishi, R.A., Liu, H., Chu, Y., Hamamura, M., Su, M.Y., Nalcioglu, O., and Anderson, A.J. (2007). Behavioral, histological, and *ex vivo* magnetic resonance imaging assessment of graded contusion spinal cord injury in mice. *J. Neurotrauma* 24, 674–689.
25. Velardo, M.J., Burger, C., Williams, P.R., Baker, H.V., Lopez, M.C., Mareci, T.H., White, T.E., Muzyczka, N., and Reier, P.J. (2004). Patterns of gene expression reveal a temporally orchestrated wound healing response in the injured spinal cord. *J. Neurosci.* 24, 8562–8576.
26. Byrnes, K.R., Fricke, S.T., and Faden, A.I. (2010). Neuropathological differences between rats and mice after spinal cord injury. *J. Magn. Reson. Imaging* 32, 836–846.
27. Day, B.W., Smith, F.M., Chen, K., McCarron, J.K., Herath, N.I., Lackmann, M., and Boyd, A.W. (2006). Eph/Ephrin membrane proteins: a mammalian expression vector pTig-BOS-Fc allowing rapid protein purification. *Protein Pept. Lett.* 13, 193–196.
28. Smith, F.M., Vearing, C., Lackmann, M., Treutlein, H., Himanen, J., Chen, K., Saul, A., Nikolov, D., and Boyd, A.W. (2004). Dissecting the EphA3/Ephrin-A5 interactions using a novel functional mutagenesis screen. *J. Biol. Chem.* 279, 9522–9531.
29. Mizushima, S., and Nagata, S. (1990). pEF-BOS, a powerful mammalian expression vector. *Nucleic Acids Res.* 18, 5322.
30. Scheff, S.W., Rabchevsky, A.G., Fugaccia, I., Main, J.A., and Lump, J.E., Jr. (2003). Experimental modeling of spinal cord injury: characterization of a force-defined injury device. *J. Neurotrauma* 20, 179–193.
31. Rossi, S.L., Nistor, G., Wyatt, T., Yin, H.Z., Poole, A.J., Weiss, J.H., Gardener, M.J., Dijkstra, S., Fischer, D.F., and Keirstead, H.S. (2010). Histological and functional benefit following transplantation of motor neuron progenitors to the injured rat spinal cord. *PLoS ONE* 5, e11852.
32. Schallert, T. (2006). Behavioral tests for preclinical intervention assessment. *NeuroRx* 3, 497–504.
33. Basso, D.M., Beattie, M.S., and Bresnahan, J.C. (1995). A sensitive and reliable locomotor rating scale for open field testing in rats. *J. Neurotrauma* 12, 1–21.
34. Rosset, A., Spadola, L., and Ratib, O. (2004). OsiriX: an open-source software for navigating in multidimensional DICOM images. *J. Digit. Imaging* 17, 205–216.
35. Wang, R., Benner, T., Sorensen, A.G., and Wedeen, V.J. (2007). Diffusion Toolkit: a software package for diffusion imaging data processing and tractography. *Proc. Intl. Soc. Mag. Reson. Med.* 15, 3720.
36. Anseloni, V.C., Ennis, M., and Lidow, M.S. (2003). Optimization of the mechanical nociceptive threshold testing with the Randall–Selitto assay. *J. Neurosci. Methods* 131, 93–97.
37. Fleming, S.M. (2009). Behavioral outcome measures for the assessment of sensorimotor function in animal models of movement disorders. *Int. Rev. Neurobiol.* 89, 57–65.
38. Cruz-Orengo, L., Figueroa, J.D., Velazquez, I., Torrado, A., Ortiz, C., Hernandez, C., Puig, A., Segarra, A.C., Whittemore, S.R., and Miranda, J.D. (2006). Blocking EphA4 upregulation after spinal cord injury results in enhanced chronic pain. *Exp. Neurol.* 202, 421–433.
39. Dries, J.L., Kent, S.D., and Virag, J.A. (2011). Intramyocardial administration of chimeric ephrinA1-Fc promotes tissue salvage following myocardial infarction in mice. *J. Physiol.* 589, 1725–1740.
40. Dobrzanski, P., Hunter, K., Jones-Bolin, S., Chang, H., Robinson, C., Pritchard, S., Zhao, H., and Ruggeri, B. (2004). Antiangiogenic and antitumor efficacy of EphA2 receptor antagonist. *Cancer Res.* 64, 910–919.
41. Iwasato, T., Katoh, H., Nishimaru, H., Ishikawa, Y., Inoue, H., Saito, Y.M., Ando, R., Iwama, M., Takahashi, R., Negishi, M., and Itohara, S. (2007). Rac-GAP alpha-chimerin regulates motor-circuit formation

- as a key mediator of EphrinB3/EphA4 forward signaling. *Cell* 130, 742–753.
42. Schucht, P., Raineteau, O., Schwab, M.E., and Fouad, K. (2002). Anatomical correlates of locomotor recovery following dorsal and ventral lesions of the rat spinal cord. *Exp. Neurol.* 176, 143–153.
 43. Steeves, J.D., and Jordan, L.M. (1980). Localization of a descending pathway in the spinal cord which is necessary for controlled treadmill locomotion. *Neurosci. Lett.* 20, 283–288.
 44. Munro, K.M., Perreau, V.M., and Turnley, A.M. (2012). Differential gene expression in the EphA4 knockout spinal cord and analysis of the inflammatory response following spinal cord injury. *PLoS ONE* 7, e37635.
 45. Murai, K.K., Nguyen, L.N., Irie, F., Yamaguchi, Y., and Pasquale, E.B. (2003). Control of hippocampal dendritic spine morphology through ephrin-A3/EphA4 signaling. *Nat. Neurosci.* 6, 153–160.
 46. Van Hoecke, A., Schoonaert, L., Lemmens, R., Timmers, M., Staats, K.A., Laird, A.S., Peeters, E., Philips, T., Goris, A., Dubois, B., Anderson, P.M., Al-Chalabi, A., Thijs, V., Turnley, A.M., van Vught, P.W., Veldink, J.H., Hardiman, O., Van Den Bosch, L., Gonzalez-Perez, P., Van Damme, P., Brown, R. H. Jr, van den Berg, L.H., and Robberecht, W. (2012) EPHA4 is a disease modifier of amyotrophic lateral sclerosis in animal models and humans. *Nat. Med.* 18, 1418–1422.
 47. Metz, G.A., and Whishaw, I.Q. (2002). Cortical and subcortical lesions impair skilled walking in the ladder rung walking test: a new task to evaluate fore- and hindlimb stepping, placing, and co-ordination. *J. Neurosci. Methods* 115, 169–179.
 48. Kozlowski, P., Raj, D., Liu, J., Lam, C., Yung, A.C., and Tetzlaff, W. (2008). Characterizing white matter damage in rat spinal cord with quantitative MRI and histology. *J. Neurotrauma* 25, 653–676.
 49. Ellingson, B.M., Schmit, B.D., and Kurpad, S.N. (2010). Lesion growth and degeneration patterns measured using diffusion tensor 9.4-T magnetic resonance imaging in rat spinal cord injury. *J. Neurosurg. Spine* 13, 181–192.
 50. Nielson, J.L., Strong, M.K., and Steward, O. (2011). A reassessment of whether cortical motor neurons die following spinal cord injury. *J. Comp. Neurol.* 519, 2852–2869.
 51. Ghosh, A., Sydekum, E., Haiss, F., Peduzzi, S., Zorner, B., Schneider, R., Baltes, C., Rudin, M., Weber, B., and Schwab, M.E. (2009). Functional and anatomical reorganization of the sensory-motor cortex after incomplete spinal cord injury in adult rats. *J. Neurosci.* 29, 12,210–12,219.
 52. Gao, Y.J., and Ji, R.R. (2010). Targeting astrocyte signaling for chronic pain. *Neurotherapeutics* 7, 482–493.
 53. Wen, Y.R., Tan, P.H., Cheng, J.K., Liu, Y.C., and Ji, R.R. (2011). Microglia: a promising target for treating neuropathic and postoperative pain, and morphine tolerance. *J. Formos. Med. Assoc.* 110, 487–494.
 54. Dixon, K.J., Munro, K.M., Boyd, A.W., Bartlett, P.F., and Turnley, A.M. (2012). Partial change in EphA4 knockout mouse phenotype: loss of diminished GFAP upregulation following spinal cord injury. *Neurosci. Lett.* 525, 66–71.

Address correspondence to:

Andrew Wallace Boyd, PhD

Queensland Institute of Medical Research

Locked Bag 2000

Royal Brisbane Hospital

Herston, QLD, 4029

Australia

E-mail: Andrew.Boyd@qimr.edu.au

or

Perry Francis Bartlett, PhD

Queensland Brain Institute

QBI Building (#79)

The University of Queensland

St Lucia, QLD, 4072

Australia

E-mail: p.bartlett@uq.edu.au